

# Thermalization and many-body localization in systems under dynamic nuclear polarization

Andrea De Luca,<sup>1</sup> Inés Rodríguez Arias,<sup>1</sup> Markus Müller,<sup>2,3,4</sup> and Alberto Rosso<sup>1</sup>

<sup>1</sup>*LPTMS, CNRS, Univ. Paris-Sud, Université Paris-Saclay, 91405 Orsay, France*

<sup>2</sup>*Condensed matter theory, Paul Scherrer Institute, CH-5232 Villigen PSI, Switzerland*

<sup>3</sup>*The Abdus Salam International Centre for Theoretical Physics, 34151, Trieste, Italy*

<sup>4</sup>*Department of Physics, University of Basel, Klingelbergstrasse 82, CH-4056 Basel, Switzerland*

We study the role of dipolar interactions in the standard protocol used to achieve dynamic nuclear polarization (DNP). In the so-called spin-temperature regime, where the interactions establish an effective thermodynamic behavior in the out-of-equilibrium stationary state, we provide numerical predictions for the level of hyperpolarization. We show that nuclear spins equilibrate to the effective spin-temperature established among the electron spins of radicals, as expected from the quantum theory of thermalization. Moreover, we present an analytical technique to estimate the spin temperature, and thus, the nuclear hyperpolarization in the steady state, as a function of interaction strength and quenched disorder. This reproduces both our numerical data and experimental results. Our central finding is that the nuclear hyperpolarization increases steadily upon reducing the interaction strength (by diluting the radical density). Interestingly, the highest polarization is reached at a point where the establishment of a spin temperature is just about to break down due to the incipient many-body localization transition in the electron spin system.

## I. GENERAL INTRODUCTION

The phenomenon of many-body localization is currently attracting a lot of attention, as it touches on various fundamental aspects of quantum statistical mechanics and quantum dynamics. However, despite its theoretical and conceptual appeal, very few consequences of practical relevance for physical processes are known so far. In this paper, we address a situation where localization does play an important role. We analyze the effects of incipient many-body localization in a system of driven quantum magnets, as standardly used in preparing polarized nuclear spins. Interestingly, we find that the achieved nuclear polarization is optimized by tuning parameters very close to the localization transition, approaching it from the delocalized side, implying a practical aspect of the localization transition.

The canonical formulation of quantum statistical mechanics assumes the contact between the system and an external reservoir. For a closed system, however, the description at large times using only few macroscopic parameters, such as the temperature or the chemical potential, implicitly assumes that the system itself can act as a thermal reservoir for its constituents. Establishing the validity of this assumption and understanding the regimes where it breaks down constitute the still open problem of quantum thermalization<sup>1,2</sup>. A simple way to probe thermalization is provided by quench protocols: a closed system is left to evolve starting from a non-thermal initial state, e.g. a state with a local excess of energy. In infinite, ergodic systems the excess energy spreads and dilutes indefinitely, so that any memory of the initial imbalance is lost. If only conserved quantities are retained from the initial state, one can argue that two eigenstates which are globally similar (e.g. have the same energy), cannot be distinguished by local measurements. This im-

plies that expectation values and correlation functions of local observables in eigenstates must coincide with their values in the microcanonical ensemble, a statement which goes under the name of Eigenstate Thermalization Hypothesis (ETH)<sup>3</sup>.

However, exceptions from such thermalizing systems can occur when the considered systems are sufficiently disordered, which may induce ergodicity breaking<sup>4,5</sup> and the associated phenomenon of “many-body localization” (MBL)<sup>6,7</sup>. Recently, a variety of approaches based on perturbation theory<sup>8</sup>, exact diagonalization<sup>9</sup>, time-dependent DMRG<sup>10</sup>, renormalization group<sup>11</sup>, local integrals of motion<sup>12–14</sup> and even rigorous mathematical results<sup>15</sup>, provided independent indications of the existence of MBL phases. In this localized phase, eigenstates have a very different structure with low entanglement following an area- rather than a volume-law<sup>16</sup>. In particular they do not obey the ETH, reflecting that the quantum dynamics is not ergodic anymore: local expectation values exhibit strong fluctuations from eigenstate to eigenstate of the same energy density, since an extensive set of parameters<sup>14,17</sup> is necessary to describe the long-time dynamics.

So far only few experimental indications of many body localization have been reported, in cold atoms<sup>18</sup> and trapped ions<sup>19</sup>, where the difficulty of isolating quantum systems from a thermalizing bath can be overcome more easily than in solid matter which always hosts phonons. However, the possibility of hole burning in frustrated magnets such as LiHo<sub>x</sub>Y<sub>1-x</sub>F<sub>4</sub> and Gadolinium Gallium Garnet<sup>20</sup> suggests that quantum magnets are promising solid state systems where localization phenomena might manifest themselves over very long time scales. After all, it was the apparent absence of spin diffusion in disordered magnets<sup>21</sup> that had led Anderson<sup>6</sup> to start the investigation of localization physics over half a century ago.

Being in a localized phase is often considered interesting for quantum technological applications, since entanglement is limited, or grows only very slowly in time<sup>16,22,23</sup>. In this work, we show that being close to a localization transition is of great interest also in an entirely different domain, as it helps to achieve large nuclear hyperpolarization in quantum magnets.

In this article, we study a class of quantum magnets relevant for so-called dynamic nuclear polarization (DNP). Those magnets generically host electron spins in a more or less random spatial configuration. To achieve a hyper-polarization the system is driven externally by microwaves. Apart from their immediate interest for DNP, these systems constitute an interesting example where the approach of a localized regime impacts the *steady state* of driven systems – rather than studying eigenstates of time-independent problems. Note that in general, even in an ergodic regime with weak disorder, no simple thermodynamic description of a driven steady state can be expected. However, in the presence of weak driving and coupling with the outside world, the dephasing time of internal degrees of freedom is much faster than any other time-scale, including the one associated with the driving. Hence the density-matrix becomes essentially diagonal in the basis of the many-body eigenstates before the effect of the driving or the environment is felt. In this limit, if ETH holds for the isolated system, the driven state can nevertheless be described to a good approximation by the same set of intensive parameters as in equilibrium, however, with values that depend on the driving. In contrast, once localization occurs in the closed spin system, the steady state reflects the details of the local dynamics of the drive and a simple equilibrium-like characterization will not emerge in general. The failure of an effective equilibrium description could potentially be investigated as a fingerprint of localization physics.

In this work we present clear signatures of thermalization and many-body localization in a model describing the hyperpolarization of nuclear spins obtained via dynamic nuclear polarization (DNP)<sup>24</sup>. For a typical DNP procedure, one works with a compound doped with radicals (i.e., molecules with unpaired electrons), which is rapidly quenched to low temperatures to form a frozen, glassy matrix.<sup>25</sup> Such a compound is then exposed to a strong magnetic field  $|\vec{B}| \simeq 3$  T, put in contact with a cold reservoir at  $\beta^{-1} \simeq 1$  K (see Fig. 1 Left), and finally irradiated with microwaves. In the absence of microwave irradiation, the system reaches thermal equilibrium at the reservoir temperature  $\beta^{-1}$ : the unpaired electrons are strongly polarized ( $\sim 94\%$ ) while the nuclear spins are very weakly polarized ( $< 1\%$ ) as the nuclear Zeeman gap is about three orders of magnitude smaller than the level splitting of the electrons. In contrast, when the microwave frequency is close to the electron's Zeeman gap, the driven system of interacting electron and nuclear spins organizes into an out-of-equilibrium steady-state with a huge nuclear polarization. The hyperpolarized sample can then be dissolved at room temperature<sup>26</sup>,

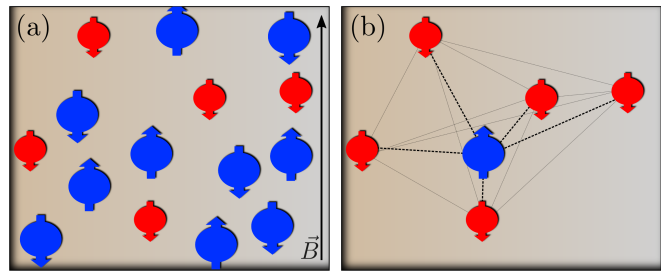


FIG. 1. Color online. Left: DNP system: the spatial positions of the nuclear spins of the compound (in blue) and the electron spins of few radical molecules (in red) are frozen in glassy matrix. The spins are coupled via dipolar and hyperfine interactions. Right: The simplified model of Eq. (9). A single nuclear spin is surrounded by a collection of electron spins. Each spin is assumed to have random interactions with all others. The electro-nuclear couplings are much weaker than the dipolar couplings connecting the electron spins among each other.

injected in patients, and used as metabolic tracer<sup>27</sup>.

The traditional explanation of hyperpolarization goes back to the seventies and is based on the idea that the spin system, when irradiated, cools down to an effective thermodynamic state characterized by a low spin-temperature<sup>24,28</sup>. This idea has been qualitatively confirmed in several experiments<sup>29,30</sup>, where the enhanced polarizations of different nuclear species ( $^{13}\text{C}$ ,  $^{15}\text{N}$ ,  $^{89}\text{Y}$ , ...) are well described by an equilibrium-like formula,

$$P_n = \tanh(\beta_s \hbar \omega_n / 2), \quad (1)$$

with a unique parameter  $\beta_s$  (the inverse spin temperature), but different Zeeman gaps  $\omega_n$  for the different species.

The success of the spin-temperature picture raises two fundamental questions:

- How can the emergence of an effective thermodynamical description be justified on a microscopic basis, and under what circumstances does an effective equilibrium indeed occur in the steady state?
- How to estimate and optimize  $\beta_s$  as a function of the microscopic parameters which can be controlled in an experiment (e.g., radical concentration, magnetic field strength, microwave intensity, ...)?

As for the first question, we will see that an effective equilibrium does not emerge in just any spin system. Rather, the thermalization tendency in the closed spin system has to be sufficiently strong in order for an effective spin temperature to establish. This in turn poses constraints on the relative strength of disorder and interactions, which can be tuned independently in experiments, as we will discuss. Previous attempts to predict the value of  $\beta_s$  were based on a purely phenomenological approach where an out-of-equilibrium quasi-thermal

state was postulated from the outset, without questioning in which parameter regime the hypothesis was actually justified. In typical experimental settings, the spin temperature was estimated to be three orders of magnitude smaller than the lattice temperature. However, the theory predicted largely unrealistic levels of hyperpolarization: up to 80%, as compared to the 20–40% observed in actual experiments<sup>31</sup>.

In a recent work, we studied an ensemble of electron spins with random Zeeman gaps and subject to dipolar interactions, but with no nuclear spins<sup>32</sup>. Under microwave irradiation and assuming a weak coupling to the reservoir, we showed that the quantum dynamics can be reduced to a master equation for the occupation probabilities of the interacting eigenstates<sup>33</sup>. For  $N = 12$  spins, the (unique) stationary state can be extracted numerically from the master equation: the steady polarizations of the electrons reflect the ergodicity properties of eigenstates. In particular we have shown that an effective spin-temperature emerges whenever: i) ETH is satisfied by the isolated spin system; ii) dephasing inside the system happens on a fast time-scale as compared to the driving and the relaxation processes involving the bath. In contrast, the signatures of a spin temperature disappear when the electron spins are many-body localized.

In this work, we study numerically the hyperpolarization of a single nuclear spin interacting with all the electron spins (see Fig. 1 Right). We show that its stationary polarization is consistent with the spin-temperature prediction of Eq. (1) when the spin Hamiltonian obeys ETH. This indicates that the steady-state parameter  $\beta_s^{-1}$  behaves as a genuine temperature. Then, in the framework of the master equation already introduced in [32], we derive a technique to estimate  $\beta_s$ . The microscopic details of the system Hamiltonian are encoded only in the equilibrium spin-spin correlation function, which can be computed analytically. The results are in good agreement both with our numerical data and, qualitatively, with experimental measurements. This paves the way to finding a set-up to optimize the hyperpolarization efficiency. We find that by decreasing the radical concentration, the spin-temperature is lowered (and hence the hyperpolarization is increased) until the stationary nuclear polarization reaches a maximal value. Below this threshold concentration an approach postulating thermalization and an effective spin-temperature would still predict a monotonous continuation of these trends. However, at this point the electron spins actually start to localize, thermalization is impeded and as a consequence the average hyperpolarization becomes strongly suppressed. The maximum efficiency in hyperpolarization is thus a fingerprint of the incipient MBL transition, which occurs as the radical concentration is reduced or the external magnetic field is increased. Since both parameters can be controlled in standard DNP experiments, these theoretical predictions can be directly subjected to experimental verification.

The paper is organized as follows: in Sec. II we in-

troduce the DNP protocol and detail how we model it. In particular we discuss how the nuclear spin is coupled to the electron spins. In Sec. III, we show how the spin temperature can be defined for the stationary state and how its value can be computed numerically and analytically; in Sec. IV we present our results while Sec. V discusses the applicability and the breakdown of the spin-temperature Ansatz as the closed system undergoes an MBL transition.

## II. THE DNP SETTING AND A SIMPLIFIED MODEL

The enhancement of the nuclear polarization emerges in the framework of a correlated quantum spin system driven far from equilibrium by resonant microwave irradiation, while being in contact with the thermal reservoir of atomic lattice degrees of freedom, held at a temperature of typically about  $T = 1\text{K}$ . Describing the dynamical behavior of such a system is a formidable task, due to several competing interactions. Below, we specify the various ingredients and derive a simplified model that can be investigated both numerically and analytically.

### A. Description of the system

In a DNP set-up, there are three fundamental ingredients: i) the internal spin dynamics governed by the competition between disorder and interactions; ii) the microwave pumping; iii) the weak contact with the reservoir. Let us describe each of them in turn.

*The spin Hamiltonian.* — The spin system is composed of the electron spins ( $S_i$ ,  $i = 1, \dots, N$ ) associated with the radical molecules, and nuclear spins ( $I_j$ , labelled  $j = 1, \dots, N_n$ ) that one aims to hyperpolarize. Typically the concentration of the nuclei is about  $N_n/N \approx 10^3$  times larger than that of the radicals. For simplicity we will consider both electron and nuclear spins to have spin  $1/2$ . All spins are exposed to a strong uniform magnetic field. The system Hamiltonian then takes the form

$$\hat{H}_S = \hat{H}_Z + \hat{H}_{\text{int}},$$

$$\hat{H}_Z = \sum_{i=1}^N (\omega_e + \Delta_i) \hat{S}_z^i - \omega_n \sum_{j=1}^{N_n} \hat{I}_z^j, \quad (2)$$

where  $\omega_e, \omega_n$  describe the average Zeeman energy of electron and nuclear spins in the external magnetic field, respectively. Because of  $g$ -factor anisotropies<sup>24</sup>, the electronic Zeeman energies are subject to spatially fluctuating contributions  $\Delta_i$ , which constitute the dominant source of quenched disorder in the problem.

The interaction term  $\hat{H}_{\text{int}}$  includes three contributions

- the dipolar interaction between electron spins, of

the form

$$\hat{H}_{e-e} = \sum_{i < j} \frac{\mu_0 \gamma_e^2}{4\pi |\mathbf{r}_{ij}|^3} \left[ \hat{\mathbf{S}}^i \cdot \hat{\mathbf{S}}^j - 3(\hat{\mathbf{S}}^i \cdot \mathbf{n}_{ij})(\hat{\mathbf{S}}^j \cdot \mathbf{n}_{ij}) \right], \quad (3)$$

where  $\mathbf{r}_{ij}$  is the distance vector between spins  $i$  and  $j$ ,  $\mathbf{n}_{ij} = \mathbf{r}_{ij}/|\mathbf{r}_{ij}|$  and  $\Gamma_e$  is the coupling constant. In a large magnetic field, this term can be regarded as a perturbation of the Zeeman energy described by (2). Therefore, hybridization between sectors of different total electronic magnetization  $\hat{S}_z = \sum_i \hat{S}_z^i$ , is strongly suppressed by the Zeeman gap. With a typical distance between radical molecules of  $r_{e-e} \simeq 20 \text{ \AA}$ , the smallness of the parameter  $\mu_0 \gamma_e^2 / r_{e-e}^3 \omega_e \simeq 10^{-3}$  justifies the secular approximation<sup>24</sup>, which projects the Hamiltonian onto these subspaces,

$$\hat{H}_{e-e} = \sum_{i < j} U_{ij} \left[ 4\hat{S}_z^i \hat{S}_z^j - (\hat{S}_+^i \hat{S}_-^j + \hat{S}_-^i \hat{S}_+^j) \right], \quad (4)$$

with  $U_{ij} = \mu_0 \gamma_e^2 (1 - 3 \cos^2 \theta_{ij}) / (16\pi |\mathbf{r}_{ij}|^3)$ . Here,  $\theta_{ij}$  is the angle between the field along  $z$  and  $\mathbf{r}_{ij}$ , and  $[\hat{S}_+^i, \hat{S}_-^i] = 2\hat{S}_z^i$ , with  $\hat{S}_\pm^i = \hat{S}_x^i \pm i\hat{S}_y^i$ .

- the dipolar interaction between nuclear spins, which takes the same form as in (3) with  $\gamma_e \rightarrow \gamma_n \simeq 10^{-3} \gamma_e$ . These interactions are responsible for nuclear spin-diffusion<sup>34</sup>, which tends to homogenize the polarization among the nuclear spins.
- the hyperfine interaction between the nuclear and the electron spins. For large Zeeman fields a projection onto  $S^z$  preserving terms yields

$$\hat{H}_{e-n} = \sum_{i,j} D_{ij}^{(z)} \hat{S}_z^i \hat{I}_z^j + D_{ij}^{(x)} \hat{S}_z^i \hat{I}_x^j + D_{ij}^{(y)} \hat{S}_z^i \hat{I}_y^j. \quad (5)$$

Note that one has the freedom to rotate the nuclear spin along the  $z$ -axis and therefore by a unitary transformation, we can always set  $D^{(y)} = 0$ . The hyperfine couplings are dominated by their anisotropic component and  $D_{ij}^{(x)} \simeq \mu_0 \gamma_e \gamma_n |r_{e-n}^{-3}|$ , with  $r_{e-n}$  the distance between electrons and nuclei. Again, the perturbative treatment is justified by the small value of the hyperfine coupling  $D_{ij}^{(x)} / \omega_e \simeq 10^{-5} \div 10^{-8}$ .

*Coupling to the lattice.* — The bath modes must be included in the Hamiltonian  $\hat{\mathcal{H}}$  of the full set-up by adding a priori two terms

$$\hat{\mathcal{H}} = \hat{H}_S + \hat{H}_R + \hat{H}_{S-R}. \quad (6)$$

Here  $\hat{H}_R$  describes the dynamics of the bath, i.e., the motion of the atoms, and  $\hat{H}_{S-R}$  captures the spin-bath interaction. The simplest description of such an interaction is obtained by assuming that each spin couples to the displacement of one individual vibrational mode

localized close to it,

$$\hat{H}_{S-R} = \lambda_e \sum_{\substack{i=1 \\ \alpha=x,y,z}}^N \hat{S}_\alpha^i \hat{\Phi}_{\alpha,e}^i + \lambda_n \sum_{\substack{j=1 \\ \alpha=x,y,z}}^N \hat{I}_\alpha^j \hat{\Phi}_{\alpha,n}^j. \quad (7)$$

Here  $\lambda_e, \lambda_n$  are the electron and nuclear spin-bath coupling constants, respectively. They fix the time-scale of the relaxation processes. Since  $\lambda_n \ll \lambda_e$ , nuclear spin-bath coupling does not play any role in the hyperpolarization procedure. As usual the specific details of the bath Hamiltonian  $\hat{H}_R$  are unimportant, its main role being to maintain the bath at temperature  $\beta^{-1} \equiv T$  and to quickly erase the memory of its past interactions with the system.

*The microwave pumping.* — The microwave frequency  $\omega_{\text{MW}}$  is tuned close to the average electronic Zeeman energy  $\omega_e$ , so that it manages to flip electron spins occasionally, one at a time. This is described by the time-dependent Hamiltonian

$$\hat{H}_{\text{MW}}(t) = 2\omega_1 \sum_i \hat{S}_x^i \cos(\omega_{\text{MW}} t), \quad (8)$$

where  $\omega_1$  is the amplitude of the microwave field.

One of the central experimental observables is the so-called DNP profile, which describes the stationary value of nuclear polarization as a function of  $\omega_{\text{MW}}$  (see Fig. 2). In order to obtain a sizeable enhancement over the thermal nuclear spin polarization, the microwave frequency  $\omega_{\text{MW}}$  must be chosen such as to lie within the range of the inhomogeneously broadened spectrum of Zeeman energies,  $(\omega_{\text{MW}} - \omega_e)^2 \lesssim \overline{\Delta_i^2}$ , so as to be resonant with a fraction of electron spin-flip transitions.

## B. Simplified model

In this article, we study a model of  $N_n = 1$  nuclear spin and  $N$  interacting electron spins, in contact with a thermal reservoir and driven out-of-equilibrium by microwave irradiation. We can limit the study to a single nuclear spin, because of an experimental fact observed under standard DNP conditions. A sample of  $^{13}\text{C}$  pyruvic acid was doped with trytil radicals, a stable and very efficient polarizing agent. The choice of trytil is such that  $\overline{\Delta_i^2} \ll \omega_n^H$ , so that hydrogen is not DNP active. In this way, the only active nuclear species is  $^{13}\text{C}$  and one observes that changing the nuclear spin concentration of  $^{13}\text{C}$  with respect to the spinless  $^{12}\text{C}$ , does not affect the final polarization of  $^{13}\text{C}$  as shown in [35]. This suggests that the enhancement in the nuclear polarizations is inherited from the steady state of the electrons and that different nuclei always have a homogeneous polarization: therefore, the study of a single nuclear spin should suffice to demonstrate the existence of a spin temperature and its transfer to the nuclear spins.

DNP is empirically found to be effective only in com-

pounds where the atoms are frozen into a random, glassy configuration in which the distances  $\mathbf{r}_{ij}$  between pairs of radicals are random. Since we will study relatively small systems, we model this in the limit of fully connected spin-spin interactions taking  $U_{ij}$  as Gaussian random variables with zero mean and variance  $U^2/N$ . Note that the simplest choice of non-fluctuating couplings  $U_{ij} = U/N$  would be pathological as it leads to the integrable Richardson model, which is always non-thermal<sup>36</sup>.

Further, we neglect the Ising coupling  $\hat{S}_z^i \hat{S}_z^j$  in (4), as it mostly modifies the instantaneous local fields seen by the various electron spins, but does not contribute essentially to the physics.

The inhomogeneous contributions to the Zeeman energy,  $\Delta_i$ , are taken equally spaced inside the interval  $[-\Delta\omega_e, \Delta\omega_e]$ <sup>37</sup>. A more realistic approximation would consider a random distribution of the  $\Delta_i$ . However this choice would lead to strong finite size fluctuations, since in the small systems accessible by numerics, at most a single electron is in resonance with the microwave irradiation.

We finally arrive at the following simplified Hamiltonian:

$$\hat{H}_S = \sum_{i=1}^N (\omega_e + \Delta_i) \hat{S}_z^i + \sum_{i < j} U_{ij} (\hat{S}_+^i \hat{S}_-^j + \hat{S}_-^i \hat{S}_+^j) - \omega_n \hat{I}_z + \sum_i D_i \hat{S}_z^i \hat{I}_x. \quad (9)$$

Here we retain only one representative term for the electron-nuclear spin coupling, which induces flips of the nuclear spin and leads to its quasi-thermalization, if the electron spins establish a spin temperature. The  $D_i$ 's are drawn from a normal distribution of zero average and variance  $D^2/N$ . The strength  $D$  is chosen so as to ensure sufficient coupling to the electrons without causing any significant perturbation of their state. The nuclear spin thus acts effectively as a thermometer.

Let us start by considering the relaxation dynamics in the absence of microwaves. In order to treat the interaction with the reservoir, we employ a significant separation of time-scales in our problem. As we observed in the previous section, the leading term in the Hamiltonian is proportional to  $\omega_e \simeq 100$  GHz in typical magnetic fields. The order of magnitude of the remaining terms of the spin Hamiltonian ( $\Delta\omega_e, U, b, \omega_n$ ) range from a few to 100 MHz. On the other hand, the rate of energy exchange with the bath can be estimated by the inverse of the electronic relaxation time,  $1/T_{1e}$ , which is of the order of 1 Hz<sup>38</sup>: this implies a *weak coupling* between electron spins and bath modes. In this limit, it is possible to derive, within the Born-Markov approximation scheme, an evolution equation for the density-matrix in Lindblad form. This approach is analogous to the equations derived by [33] and has the advantage of being directly connected to the microscopic model<sup>39</sup>. The details of this derivation were presented in [32]. Summarizing, the resulting

evolution of the density matrix of the spin system,  $\rho$ , has the Lindblad form

$$\frac{d\rho}{dt} = -i[\hat{H}_S, \rho] + \mathcal{L}[\rho]. \quad (10)$$

The last term contains the non-unitary dynamics with two kinds of contributions: i) electron spin-flip processes (due to the coupling of bath modes with  $S_x^i, S_y^i$  in (7)) which induce transitions between pairs of eigenstates of  $\hat{H}_S$  and involve an exchange of energy  $\simeq \omega_e$  with the lattice; ii) processes due to the coupling of the bath modes with  $\hat{S}_z^i$  or  $\hat{I}_z$  for which the exchange of energy vanishes in the non-interacting limit. The latter thus contributes mostly to the dephasing of off-diagonal elements of the density-matrix in the basis of eigenstates of  $\hat{H}_S$ , while the former dominates the relaxation of the diagonal elements, so that at long-times the density-matrix reaches the thermal state at the lattice temperature:  $\rho = Z^{-1} e^{-\beta \hat{H}_S}$ .

The precise estimation of the different time scales is difficult. Experimentally, one knows that  $T_{1e} \simeq 1$  s and  $T_{2e} \simeq 10^{-6}$  s, associated with the relaxation of the longitudinal and the transverse spin polarization, respectively<sup>40</sup>. Given the huge difference between the two time scales<sup>41</sup> we assumed in Ref. [32] that the quantum dynamics of the system can be reduced to a classical master equation for the occupation probabilities  $p_n$  of the many-body eigenstates  $\Psi_n$

$$\frac{dp_n}{dt} = \sum_{n' \neq n} W_{n' \rightarrow n} p_{n'} - W_{n \rightarrow n'} p_n, \quad (11)$$

where the transition rate has the form  $W_{n,n'} = W_{n,n'}^{\text{bath}}$ :

$$W_{n,n'}^{\text{bath}} = \frac{2h_\beta(\Delta\epsilon_{n,n'})}{T_{1e}} \sum_{j=1}^N \sum_{\alpha=x,y,z} |\langle n | \hat{S}_\alpha^j | n' \rangle|^2, \quad (12)$$

Eq. (12) describes spin-flips induced by the interaction with the external bath on a time scale  $T_{1e}$  and the function  $h_\beta(x) = e^{\beta x} / (1 + e^{\beta x})$  assures detailed balance and convergence to Gibbs equilibrium at temperature  $\beta^{-1} \equiv T \simeq 1$  K. The coupling of the nuclear spin to the bath modes induces similar transitions but with a much smaller rate as  $T_{1n} \gtrsim 10^3 T_{1e}$ . We remark that a single electron spin would dephase also in absence of the external reservoir due to dipolar coupling with the other spins. In particular, in the ergodic phase, the system can act as its own reservoir and there is an internal notion of dephasing: the experimental  $T_{2e}$  is affected by the internal one, but for simplicity treat it as a separate input parameter independent of the interaction strength  $U$ .

We now include the coupling to the microwave radiation as described by (8). As the microwave field is time-dependent, it requires some care. A precise estimation of the microwave amplitude  $\omega_1$  is difficult, since it is hard to evaluate the fraction of emitted power which actually reaches the sample in a given experiment. In general, we

can assume that  $\omega_1$  is within the range of tens to hundreds of kHz. Thus, the transition rate satisfies  $\omega_1^2 T_{2e} \ll \omega_e$ . Together with the condition  $\Delta\omega_e \ll \omega_e$  this ensures that we can safely employ the well-known *rotating-wave approximation*: It entails transforming the Hamiltonian and the density-matrix into a rotating frame, i.e.,

$$\rho^{(r)} = e^{i\hat{S}_z\omega_{\text{MW}}t} \rho e^{-i\hat{S}_z\omega_{\text{MW}}t}, \quad (13)$$

$$\text{Tr}[\hat{O}\rho] = \text{Tr}[e^{-i\hat{S}_z\omega_{\text{MW}}t} \hat{O} e^{i\hat{S}_z\omega_{\text{MW}}t} \rho^{(r)}], \quad (14)$$

where the last line holds for any observable  $\hat{O}$ , and  $\hat{S}_\alpha = \sum_i \hat{S}_\alpha^i$ . For observables that commute with  $\hat{S}_z$ , such as the individual polarizations  $\hat{S}_z^i$ , expectation values can safely be computed in the rotating frame. The advantage of the transformation (13) is that, since  $[\hat{S}_z, \hat{H}_S] = 0$ , the evolution of  $\rho^{(r)}$ , in the presence of microwaves, is the same as that for  $\rho$  in (10), where, apart from rapidly oscillating terms, the Hamiltonian has been replaced by the time-independent

$$\hat{H}_S^{\text{rot}} \rightarrow \hat{H}_S - \omega_{\text{MW}}\hat{S}_z + \omega_1\hat{S}_x \quad (15)$$

while  $\mathcal{L}[\rho] \rightarrow \mathcal{L}[\rho^{(r)}]$ . Within this approximation the effect of microwaves can be included in the master equation (11) as an additional rate  $W_{n,n'} = W_{n,n'}^{\text{bath}} + W_{n,n'}^{\text{MW}}$ , with

$$W_{n,n'}^{\text{MW}} = \frac{4\omega_1^2 T_{2e} |\langle n | \hat{S}_x | n' \rangle|^2}{1 + T_{2e}^2 (|\epsilon_n - \epsilon_{n'}| - \omega_{\text{MW}})^2}. \quad (16)$$

Again, the use of the master equation is justified as long as  $\omega_1^2 T_{2e}$  is small as compared to the amplitude of the intra-spin interaction terms.

It is important to observe that for  $\omega_1 \neq 0$ , the rates  $W_{n,n'}$  do not respect a detailed balance condition and thus, the stationary state will be out-of-equilibrium.

### III. THE SPIN-TEMPERATURE ANSATZ FOR THE STATIONARY STATE

In this section we discuss the behavior of the system ignoring the nuclear spin, which is weakly coupled and serves only as a thermometer, without acting back on the electronic system. The time evolution of the spin system can be decomposed into two regimes. At rare times, the thermal reservoir or the microwave field flips a single electron spin. Subsequently, fast dephasing brings the system essentially into a classical mixture of eigenstates of  $\hat{H}$  (this is a good description as far as local observables are concerned). Since the spin-flip is a perturbation localized in space, it is natural to ask how much information about the position of the flipped spin is retained after dephasing. As long as the electron spins form an ergodic system no local information except for the increment of the conserved quantities (energy and electron spin polarization) will remain. It implies that after the typical dephasing time, for any local observable, the expectation

value on the projected state coincides with the average over all states characterized by the same value of energy and electron polarization. In a canonical description this corresponds to the equilibrium average in presence of two intensive parameters:

$$p_n \simeq p_n^{\text{Ans}} = Z^{-1} e^{-\beta_s(\epsilon_n + h s_{z,n})}, \quad (17)$$

where  $Z$  is fixed by normalization. The inverse spin-temperature,  $\beta_s$ , is the parameter conjugate to the energy, while the effective magnetic field,  $h$ , is conjugate to the electron magnetization:  $\epsilon_n$  and  $s_{z,n}$  are the eigenvalues of  $\hat{H}$  and  $\hat{S}_z$  on  $|n\rangle$  in the laboratory (non-rotating) frame. In the following we compute both parameters following two complementary approaches:

- A fitting method (FM), which allows us to infer  $\beta_s$  and  $h$  from numerical simulations, by imposing that the distribution  $p_n^{\text{Ans}}$  in (17) has the exact average energy and electron magnetization.
- A perturbative expansion (PE) for weak  $U$  and for an infinite number of spins interacting via (9). This method is based on the observation that the variation of energy and electron polarization, induced by single spin flip transitions, are encoded in the spin-spin correlation functions computed with the density-matrix at time  $t$ . Using (17), these functions can be computed, at least order by order in perturbation theory in  $U$ . The values of  $\beta_s$  and  $h$  can then be determined by imposing a balance for the total in- and outflow of energy and electron spin polarization due to interactions with the radiation and the bath. Note that the thermal average of correlation functions is only weakly affected by localization at small  $U$  and therefore perturbation theory can produce sensible results.

We now explain the details of the two procedures.

#### A. Fitting method

Our fitting method allows us to fix the parameters of the spin-temperature Ansatz for a given value of  $U$ . We use a numerical simulation to obtain the stationary state of Eq. (11) in a given realization of the couplings  $U_{ij}$  and  $D_i$ . First, by exact diagonalization of the Hamiltonian  $\hat{H}$ , we compute the  $2^{N+1}$  eigenstates  $|n\rangle$  of energy  $\epsilon_n$  and total electron polarization  $s_{z,n}$ . The exponential growth of the Hilbert space strongly limits the accessible sizes, and thus we restrict ourselves to  $N = 12$ . The rates in Eqs. (12, 16) can be computed exactly as matrix elements between pairs of eigenstates. Then, the occupation probabilities in the stationary state  $p_n^{\text{stat}}$  are obtained by setting  $dp_n/dt = 0$  in Eq. (11) and solving the resulting linear system. Typically there is a unique solution to these equations, both in the ergodic and the localized phases of the isolated system. In particular there is no

memory of the initial state in the localized phase. This is an important difference with respect to the dynamics of closed many-body localized systems, which retain infinitely long lived memory of the initial state.

Under the hypothesis of Eq. (17) for ergodic phases, a natural way to fix the two parameters  $\beta_s$  and  $h$  is based on matching the expectation values of the two conserved quantities, i.e., requiring

$$\overline{\langle \hat{H} \rangle}_{\text{stat}} = \overline{\langle \hat{H} \rangle}_{\text{Ans}}, \quad (18a)$$

$$\overline{\langle \hat{S}_z \rangle}_{\text{stat}} = \overline{\langle \hat{S}_z \rangle}_{\text{Ans}}. \quad (18b)$$

Here the overline represents the average over the different realizations and  $\langle \hat{O} \rangle_{\text{stat}} = \sum_n p_n^{\text{stat}} \langle n | \hat{O} | n \rangle$  and similarly  $\langle \hat{O} \rangle_{\text{Ans}} = \sum_n p_n^{\text{Ans}} \langle n | \hat{O} | n \rangle$ . In Eq. (18), the values of  $s_{z,n}$ ,  $\epsilon_n$  and  $p_n^{\text{stat}}$  are obtained numerically for each realization. Instead, the parameters  $\beta_s^{\text{FM}}$  and  $h^{\text{FM}}$  take realization-independent values which can be solved, e.g., by using Newton's method.

## B. Perturbative expansion for weak interactions

A different estimation of the quasi-equilibrium parameters is based on the time-evolution of the total energy and magnetization. Indeed, since these two quantities are conserved by  $\hat{H}_S$ , their values merely change due to the spin-flip transitions induced by the reservoir and the microwave field. All the microscopic details are then encoded in the spin-spin correlation function, that at large times, writes as (see Appendix A)

$$\chi_{ij}(u, v) = \sum_n p_n^{\text{stat}} \langle n | U(u, v) \hat{S}_x^i U^\dagger(u, v) \hat{S}_x^j | n \rangle \quad (19)$$

with  $U(u, v) = e^{i(\hat{H}_S u + \hat{S}_z v)}$ . If the spin-temperature Ansatz (17) holds,  $\chi_{ij}(u, v)$  reduces to the calculation of the spin-spin correlation function at equilibrium (see Appendix B). Since, at stationarity, the total exchange of magnetization and energy must vanish, we obtain two conditions, which in the limit of negligible interaction strength  $U$  can be written explicitly as (see Appendix C)

$$\int d\omega f(\omega) \kappa(\omega) = 0, \quad (20a)$$

$$\int d\omega \omega f(\omega) \kappa(\omega) = 0. \quad (20b)$$

Hereby  $f(\omega) = \frac{1}{N} \sum_i \delta(\omega_e + \Delta_i - \omega)$  is the distribution of the Zeeman energies of the electron spins, which we, at large  $N$ , chose to be uniform in  $[\omega_e - \Delta\omega_e, \omega_e + \Delta\omega_e]$ ;  $\kappa(\omega) \equiv \frac{dP_e(\omega)}{dt}$ , describes the rate of change of polarization (due to radiation and reservoir) of the spins with

Zeeman energy  $\omega$ , i.e.

$$\kappa(\omega) = \frac{P_0(\omega) - P_e(\omega)}{2T_{1e}} - \frac{T_{2e}\omega^2 P_e(\omega)}{T_{2e}^2(\omega - \omega_{\text{MW}})^2 + 1}. \quad (21)$$

where  $P_0(\omega) = -\tanh(\beta\omega/2)$  is the equilibrium polarization in the absence of microwaves. In the absence of interactions the electron polarization  $P_e(\omega)$  is fixed by  $\kappa(\omega) = 0$ , as different frequencies do not mix. However, the spin-temperature Ansatz assumes the expression  $P_e(\omega) = -\tanh(\beta_s(\omega + h)/2)$  in the steady state: a non-zero value of  $\kappa$  at specific  $\omega$  is of course compensated by the interaction-mediated redistribution of the conserved quantities among the spins. In Eq. (21), the first accounts for the relaxation of polarization due to the reservoir, while the second term captures the effect of the microwave field. A very similar form of  $\kappa$  was proposed by Borghini<sup>31</sup>:

$$\kappa_{\text{Borg}}(\omega) = \frac{P_0(\omega) - P_e(\omega)}{2T_{1e}} - \pi\omega^2 P_e(\omega) \delta(\omega - \omega_{\text{MW}}), \quad (22)$$

in which the Lorentzian absorption in (21) was replaced with an infinitely sharp  $\delta$ -function, assuming that only electron spins in exact resonance with  $\omega_{\text{MW}}$  are flipped by the microwaves. This leads, however, to a substantial underestimation of the spin-temperature<sup>42,43</sup> as compared to the experimentally observed values.

Our formula in Eq. (21) instead yields values closer to experimental observations for  $\beta_s^{\text{PE}}, h^{\text{PE}}$ . Moreover, we can extend Eq. (20) to finite  $U$  and take into account perturbative corrections for  $U \ll \Delta\omega_e$ . They take the form (see Appendix C):

$$\int d\omega f(\omega) \left[ \kappa(\omega) + \frac{U^2}{2} \int d\omega' f(\omega') \kappa_1(\omega, \omega') \right] = 0, \quad (23a)$$

$$\int d\omega f(\omega) \left[ \omega \kappa(\omega) + \frac{U^2}{2} \int d\omega' f(\omega') \kappa_2(\omega, \omega') \right] = 0, \quad (23b)$$

where the second-order corrections are given by

$$\kappa_1(\omega, \omega') = \frac{d}{d\omega} \left( \frac{\kappa(\omega) - \kappa(\omega')}{\omega - \omega'} \right), \quad (24)$$

$$\kappa_2(\omega, \omega') = \frac{d}{d\omega} \left( \frac{\omega \kappa(\omega) - \omega' \kappa(\omega')}{\omega - \omega'} \right). \quad (25)$$

## IV. NUMERICAL RESULTS

We focus on the standard conditions of DNP experiments using trytills for the hyperpolarization of  $^{13}\text{C}$  nuclear spins. The value of the microscopic parameters are taken from actual experiments and summarized in Table I.

The aim of this section is twofold: on the one hand,

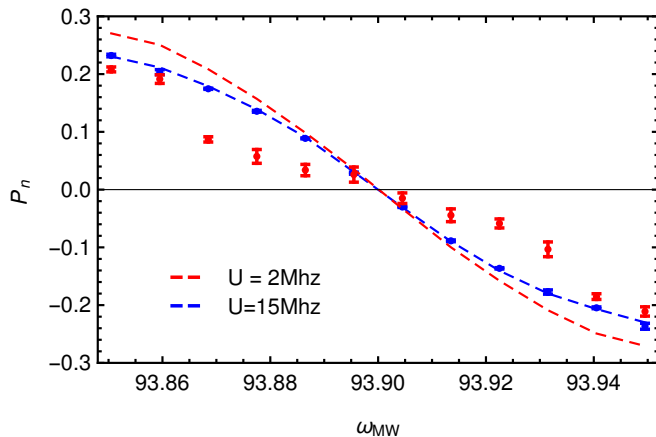


FIG. 2. Color Online. **The DNP profile**, i.e. the steady state value of the nuclear polarization as a function of the microwave frequency. In red we show the results for  $U = 2$  MHz, in blue the results for  $U = 15$  MHz. Symbols correspond to the steady state value of the nuclear polarization, while the dashed line corresponds to Eq. (1) with  $\beta_s$  obtained with the fitting method.

$T_{1e}$	$T_{2e}$	$\vec{B}_0$	$\beta$	$U$
1. s	$10^{-6}$ s	3.35 Tesla	$0.83 \text{ K}^{-1}$	$2.0 \div 45.0 \text{ MHz}$
$\omega_e$	$\Delta\omega_e$	$\omega_1$	$\omega_n$	
93.9 2 $\pi$ GHz	54 2 $\pi$ GHz	$0.25 \times 10^{-4}$ 2 $\pi$ GHz	20 2 $\pi$ MHz	

TABLE I. Summary of the parameters used in our calculations.

we test the range of validity of the spin-temperature assumption for the stationary state; on the other hand, we quantify the finite-size correction affecting our numerical results for  $N = 12$  (averaged over at least 100 configurations). To achieve this, we focus on the stationary nuclear spin polarization. The nuclear spin is weakly coupled with the electron spins and acts simply as a thermometer; within the spin-temperature Ansatz, its stationary polarization is therefore expected to take the form of Eq. (1). We can then compare three different estimations for  $P_n$ :

- the value predicted by Eq. (1), with  $\beta_s = \beta_s^{\text{FM}}$  as obtained from the fitting method explained in Sec. III A;
- the value predicted by Eq. (1), with  $\beta_s = \beta_s^{\text{PE}}$ , obtained from the perturbative expansion in the thermodynamic limit  $N \rightarrow \infty$  of the fully-connected model, as explained in Sec. III B;
- the exact value obtained upon averaging over several realizations the stationary nuclear spin polarization obtained from the numerical procedure over

several realizations

$$P_n = \sum_m p_m^{\text{stat}} \langle m | I_z | m \rangle. \quad (26)$$

In Fig. 3 the dashed lines are the prediction for the nuclear polarization with the analytical estimates for the spin-temperature. For small interaction, the perturbative results of Eqs. (23) are in good agreement with the numerical data. Upon increasing  $U$ , the lowest order result Eq. (23) cannot be expected to be accurate anymore, but it still correctly describes the decrease in polarization, and thus captures the important, but hitherto unexplained, effect of radical concentration seen in the experiments<sup>26,35</sup>: as the radical concentration, and thus  $U$ , is increased, the nuclear polarization decreases.

On the left of Fig. 3, we show the behavior of the nuclear hyperpolarization as a function of the dipolar coupling  $U$ , at fixed disorder strength. We observe two regimes: in the strongly-interacting regime, the concept of a spin-temperature perfectly applies to the stationary states and the polarization of the nuclear spin collapses with the prediction given by (1) and  $\beta_s = \beta_s^{\text{FM}}$ . For  $U \lesssim 10$  MHz, ( $U/\Delta\omega_e \lesssim 0.2$ ) the observed polarization is much smaller than the value expected by postulating a spin-temperature state of the electrons. This shows that at least for our finite  $N$  simulations, the thermal regime breaks down. We expect that this behavior remains true in the thermodynamic limit of systems with a finite connectivity among electron spins. A similar behavior is observed in the right panel of Fig. 3, where the magnetic field is varied at constant interaction strength  $U$ . We recall that the disorder strength, i.e., the spread of inhomogeneous contributions to the Zeeman energies,  $\Delta\omega_e$ , increases proportionally with the external magnetic field  $|\vec{B}|$ . Thus, at small fields the dominating interactions establish a spin-temperature, whereas at large fields, the internal thermalization of the electron system breaks down. We note that both methods to compute the spin-temperature, the fitting procedure for  $N = 12$  systems and the perturbative analytical calculation for a mean field ( $N = \infty$ ) system, yield compatible results. Their difference seems to stem mostly from the error due to the restriction of the perturbative calculation to quadratic order in  $U$ , rather than due to the effects of comparing  $N = 12$  with the mean field limit  $N = \infty$ .

In Fig. 2, we show an important characteristics of a DNP experiment, known as the DNP profile: the hyperpolarization as a function of the irradiated microwave frequency  $\omega_{\text{MW}}$ . We compare the exact value of  $P_n$  from (26) with the prediction from the fitting method and plugging  $\beta^{\text{FM}}$  into (1). For  $U = 15$  MHz ( $U/\Delta\omega_e \simeq 0.3$ ), the two results are consistent, while for  $U = 2$  MHz ( $U/\Delta\omega_e \simeq 0.04$ ), we generally observe a small hyperpolarization, with the exception of the a window of width  $O(\omega_n)$  around  $\omega_{\text{MW}} = \omega_e \pm \Delta\omega_e$ , where the polarization is induced by the so-called solid effect<sup>44</sup>. The latter consists in the following: Even in the absence of dipolar interac-



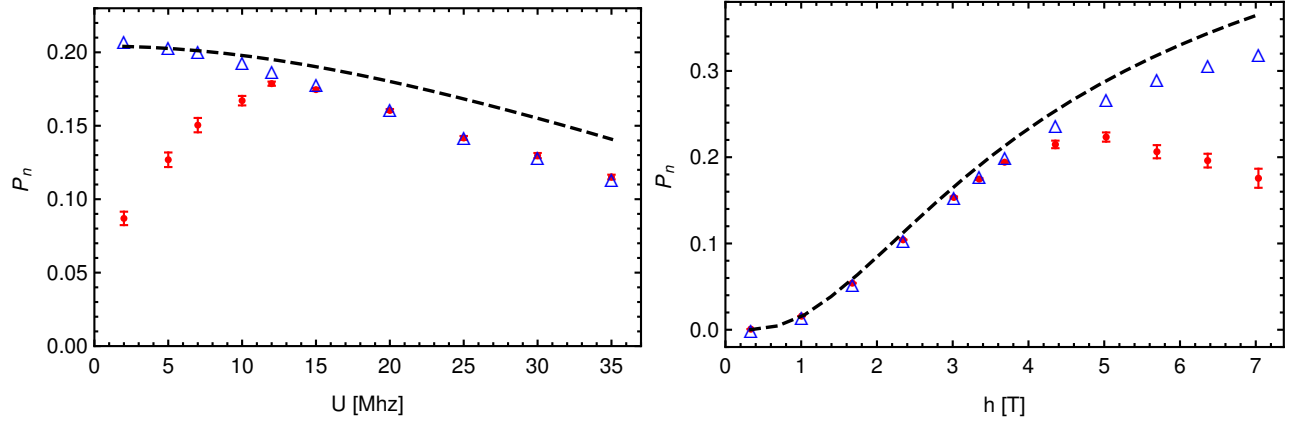


FIG. 3. **Breakdown of the existence of a spin-temperature.** The steady state polarization of the nuclear spin is plotted as a function of the typical dipolar coupling strength  $U$  at a fixed magnetic field  $B = 3.35$  Tesla (Left) and as a function of the magnetic field  $B$  at fixed  $U = 15$  Mhz (Right). The red disks show the nuclear polarization in the stationary state averaged over many realizations (the error bar shows the standard deviation). These results are compared with values of the nuclear polarization obtained from Eq. (1). The blue triangles correspond to a spin temperature,  $\beta_s^{-1}$  estimated by the fitting method of (18) while the black dashed line corresponds to the perturbative expansion discussed in Sec. IIIB. Both plots show the breakdown of the spin-temperature assumption once the spread of Zeeman inhomogeneities dominates over the strength of the dipolar interactions.

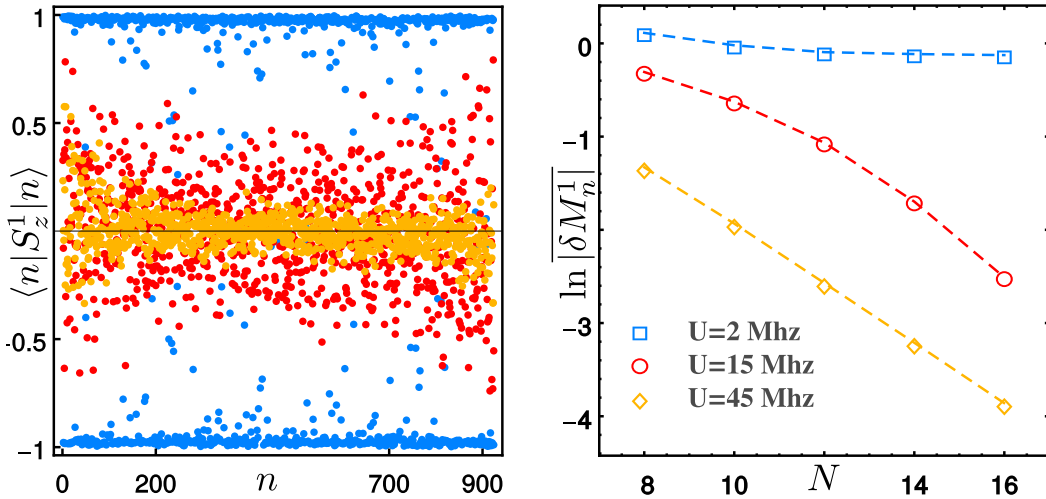


FIG. 4. Color online. Numerical investigation of the ETH hypothesis for a system of  $N$  electron spins. (a) Average polarization of the selected spin  $\hat{S}_z^1$  in the eigenstates  $|n\rangle$  of  $N = 12$  electron spins with vanishing total magnetization. The  $|n\rangle$  are ordered according to increasing energy. Data are shown for three different values of the dipolar strength:  $U = 2$  MHz (blue), 15 MHz (red), 45 MHz (blue);  $\Delta\omega_e = 54$  MHz. (b) Difference in local magnetization between consecutive eigenstates,  $\delta M_n^1 = \langle n+1 | \hat{S}_z^1 | n+1 \rangle - \langle n | \hat{S}_z^1 | n \rangle$ , averaged over disorder realizations and globally unpolarized eigenstates, for different system sizes  $N = 8, \dots, 16$ . An exponential decay of  $\delta M_n^1$  with  $N$  indicates a thermal phase obeying ETH, while a saturation signals many-body localization.

tions among the electrons, the presence of hyperfine interactions allows the microwaves to excite an prohibited transition, where the nuclear spin is flipped together with an electron with a transition frequency  $\omega_i = \omega_{\text{MW}} \pm \omega_n$ . This effect is more prominent at the boundaries of the microwave spectrum of interest,  $\omega_{\text{MW}} \in [\omega_e - \Delta\omega_e, \omega_e + \Delta\omega_e]$ . Indeed, in the bulk of the spectrum simultaneous flips of an electron and a nuclear spin have similar probability,

and therefore their effects tend to cancel.

## V. DISCUSSION

As discussed in the previous section, the data presented in Fig. 3 indicate a marked change of behavior for weak dipolar couplings (i.e., for low radical concentra-

tion) and/or in large magnetic fields. Since the hyperfine interaction between the nuclei and the electrons is left unchanged in both these cases, this phenomenology actually reflects a change in the electron system. Indeed, in order for the electron spins to act as a bath for the nucleus, they have to be in a "thermal phase". Upon decreasing the value of  $U$ , the disorder in the inhomogeneous Zeeman energies,  $\Delta\omega_e$ , becomes dominant: the eigenstates fail to be ergodic and enter a many-body localized phase. Indications of this transition are shown in Fig. 4 where we study the expectation value of the polarization of a selected electron spin, say  $S^1$ , on all eigenstates within the sector of vanishing total electron polarization:  $\langle n | \hat{S}_z^1 | n \rangle$ . The left of Fig. 4 visualizes the qualitatively different behaviors for weak and strong interactions, respectively, in a single realization, at fixed magnetic field  $B = 3.35$  Tesla: At weak interactions  $U \simeq 2$  MHz ( $U/\Delta\omega_e \simeq 0.04$ ), the expectation value  $\langle n | \hat{S}_z^1 | n \rangle$  fluctuates between the fully polarized extremes  $\pm 1/2$ . In contrast, when the interactions dominate,  $U \simeq 15, 45$  MHz, ( $U/\Delta\omega_e \simeq 0.3, 0.8$ ), the values of  $\langle n | \hat{S}_z^1 | n \rangle$  instead concentrate close to the equilibrium value 0. This difference becomes sharper and sharper with increasing system size, as analyzed by the average variations of the local magnetization as a function of  $N$ , c.f. the right panel of Fig. 4. The extrapolation of such data to the thermodynamic limit allows one to locate the many-body localization transition. The data confirm that at strong interactions  $U$  there is a thermal phase obeying ETH. This is exemplified by the expectation values of the local observable  $S_z^1$  which coincide for all eigenstates and agree with the thermodynamic average. In contrast, for small  $U$  and the accessible system sizes, we observe the fingerprints of many-body localization, with strong fluctuations of local observables between different eigenstates. In this case, thermodynamic expectation values can only be recovered by averaging over many eigenstates.

Internal thermalization among the electron spins explains the emergence of an effective spin-temperature in DNP experiments, as long as the thermalization is much faster than the driving and bath relaxation processes. In the ergodic phase this is essentially always the case, given that the latter given that the latter are orders of magnitude slower than the internal spin dynamics. Indeed, the thermal eigenstates cannot encode any memory about local perturbations such as the frequency-selective spin-flips driven by the microwave radiation. In contrast, in the localized phase, there exists an extensive set of local conserved quantities in the isolated system. This implies that two parameters  $\beta_s$  and  $h$  cannot contain sufficient information to describe local observables in all eigenstates of given total energy and polarization. As a consequence, the steady state and its properties will be more complex, and depend on details of how the radiation and the bath couple to individual spins, and how those are coupled among each other. Our numerical results show that the steady state concentrates on eigenstates with a vanishing polarization of resonant electron spins and a strong

polarization of the non-resonant ones.

The dependence of the nuclear spin polarization (via the spin temperature) on interaction strength and magnetic field, as shown in Fig. 3, can be understood, at least at a qualitative level. Indeed, when the ratio between interactions and magnetic field,  $U/B$ , is increased, two competing effects are enhanced simultaneously:

- The tendency towards thermalization increases, which eventually leads to ETH and the appearance of the spin-temperature;
- The microwave irradiation is effective on a larger number of spins and thus acts less selectively. Indeed, all spins with Zeeman gap satisfying  $|\omega_e + \Delta_i - \omega_{MW}| = T_{2e} + O(\delta E(U))$  will absorb the microwave irradiation efficiently. Hereby,  $\delta E(U) \simeq \min[U^2/\Delta\omega_e, U]$  is the interaction-induced width of the local spectral functions of typical spins. The associated broadening of the absorption line implies a broader range of spins with suppressed polarization in the steady state, and thus an increase in the resulting spin temperature

In practice, while a sufficiently large  $U$  is needed to ensure thermalization among the electron spins, too large a value broadens the absorption line, which ultimately results in a stationary state with a higher spin temperature. Therefore, we reach the conclusion that the inverse spin temperature, and thus the achieved hyperpolarization level of nuclear spins, will reach a maximal value when  $U/B$  is tuned to the proximity of the many-body localization transition: There, thermalization still occurs, but the microwave irradiation couples to spins in a maximally narrow frequency range, enabling a low spin temperature to emerge.

Additional insights of the validity or failure of the spin-temperature Ansatz for different values of  $U$  are provided in Fig. 5. It is possible to give a quantitative estimation of the validity of the Ansatz in (17) using a standard statistical indicator, known as Kullback-Leibler divergence. It quantifies the amount of information loss when  $p_n^{\text{Ans}}$  is used to approximate  $p_n^{\text{stat}}$  and is defined as

$$D_{KL} = \sum_n \ln \left( \frac{p_n^{\text{stat}}}{p_n^{\text{Ans}}} \right) p_n^{\text{stat}} \quad (27)$$

The average of  $D_{KL}$  over disorder realizations is shown in Fig. 5 left, as a function of the dipolar coupling. For small values of  $U$ , the large value of  $D_{KL}$  reflects the fact that the spin-temperature Ansatz cannot reproduce accurately the local behavior of the spin-polarizations. At large  $U$ , where the spin-temperature picture applies, the value of  $D_{KL}$  becomes much smaller. An interesting question is whether a small but finite difference always remains in the thermodynamic limit, i.e. if with an appropriate observable the stationary state could be distinguished from thermal ensemble.

A fingerprint of the localization transition is seen in the sample-to-sample fluctuations of the stationary nu-

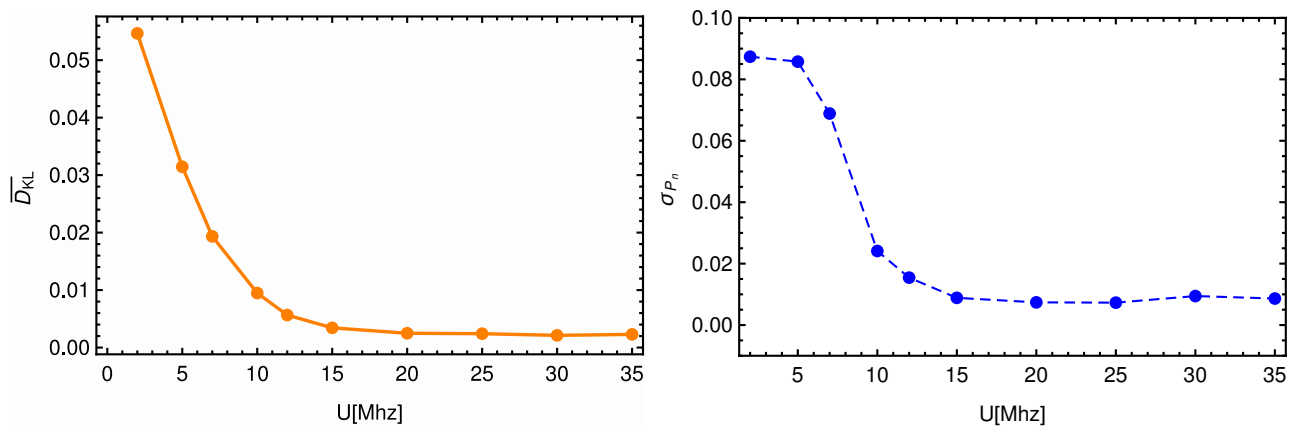


FIG. 5. (a) The Kullback-Leibler divergence, comparing the distribution in the stationary state  $p_n^{\text{stat}}$  with the spin-temperature Ansatz  $p_n^{\text{Ans}}$  of (17). (b) The sample-to-sample fluctuations of the nuclear polarization as a function of  $U$ . The localized phase is characterized by vastly enhanced fluctuations of the polarization of the probing nuclear spin, demonstrating the absence of a homogeneous spin temperature in the electronic system.

clear polarization shown in Fig. 5 right. In the thermal phase, fluctuations originate only from the finite-size effects on the total energy and magnetization in the stationary state and are therefore largely suppressed. In the localized phase instead, local processes control the nuclear polarization and the final polarization depends on the presence or absence of few-body resonances.

## VI. CONCLUSION

We presented a simple model for an improved description of DNP, which accounts for the crucial role played by dipolar interactions among radical spins. For sufficiently strong dipolar coupling, the electron spin system thermalizes internally and acts as an effective thermal bath for the nuclear spins and cools them down to the spin-temperature established among the electron spins. For this regime, we analytically estimated the achieved nuclear spin polarization in a perturbative expansion in the dipolar coupling, which we nevertheless assume strong enough to ensure a thermal phase.

In that phase the maximal hyperpolarization in DNP is obtained by minimizing the effective spin temperature. Our analysis shows that this is achieved by reducing the interaction strength to maximal possible extent, that is upon approaching the localization transition from the ergodic phase. This can be achieved by either reducing the radical concentration or increasing the magnetic field strength. The localized phase of the electron spins instead yields a significantly lower degree of nuclear spin polarization. Here a word of caution qualifying the meaning of many-body localization in real dipolar systems is in order. A genuine localization transition in the isolated system at finite energy density is expected only if the interactions are sufficiently short range. For dipolar interactions, already Anderson's work<sup>6</sup> suggested delocalization, even though on exponentially long time scales, as

$U/\Delta\omega_e$  becomes small. This is because dipolar couplings decay as a marginal power law, which always allow spins to find resonant partners at large distance. Even in  $d = 2$  dimensions it has been argued that there are channels for delocalization<sup>45,46</sup>, with however, even longer time scales. When invoking a localization transition, we in fact allude to a strong crossover to very long thermalization time scales which grow exponentially with  $\Delta\omega_e/U$ . The latter makes the spin temperature Ansatz break down rather quickly, too. Similarly, the mean field model is not expected to have a genuine localization transition as  $N \rightarrow \infty$ , which further justifies a posteriori our expansion around the non-interacting limit. Nevertheless, a thorough understanding of the thermalization processes and the involved time scales in the limit  $N \rightarrow \infty$  require further analysis.

It would be interesting to test these predictions in standard experimental DNP set-ups, both to validate our conclusions and to investigate the manifestation of the many-body localization transition in out-of-equilibrium stationary states.

It will be important to understand the crossover to a regime where the driving is eventually faster than the dephasing and/or the internal equilibration times, so that hole-burning phenomena and saturation of the driving efficiency become important. Furthermore, one should understand more thoroughly the localization transition as a function of the effective connectivity of the electron spins, which presumably varies with their dilution and the associated positional randomness in the radical spins. The latter presumably varies with the dilution of radicals and their positional randomness. We plan to address these issues in a future publication.

## ACKNOWLEDGMENTS

This work is supported by “Investissements d’Avenir” LabEx PALM (ANR-10-LABX-0039-PALM). We thank

L. Mazza and Xiangyu Cao for interesting discussions, S. Colombo Serra for the support with experimental data and C. Zankoc for collaboration in the early stage of this work.

- 
- <sup>1</sup> M. Rigol, V. Dunjko, and M. Olshanii, *Nature* **452**, 854 (2008).
  - <sup>2</sup> A. Polkovnikov, K. Sengupta, A. Silva, and M. Vengalattore, *Rev. Mod. Phys.* **83**, 863 (2011).
  - <sup>3</sup> J. Deutsch, *Physical Review A* **43**, 2046 (1991); M. Srednicki, *Physical Review E* **50**, 888 (1994).
  - <sup>4</sup> A. De Luca and A. Scardicchio, *Europhys. Lett.* **101**, 37003 (2013).
  - <sup>5</sup> A. De Luca, B. L. Altshuler, V. E. Kravtsov, and A. Scardicchio, *Phys. Rev. Lett.* **113**, 046806 (2014).
  - <sup>6</sup> P. W. Anderson, *Phys. Rev.* **109**, 1492 (1958).
  - <sup>7</sup> R. Nandkishore and D. A. Huse, *Annual Review of Condensed Matter Physics* **6**, 15 (2015), arXiv:1404.0686 [cond-mat.stat-mech].
  - <sup>8</sup> D. Basko, I. Aleiner, and B. Altshuler, *Ann. Phys.* **321**, 1126 (2006).
  - <sup>9</sup> A. Pal and D. A. Huse, *Phys. Rev. B* **82**, 174411 (2010).
  - <sup>10</sup> J. H. Bardarson, F. Pollmann, and J. E. Moore, *Phys. Rev. Lett.* **109**, 017202 (2012).
  - <sup>11</sup> R. Vosk and E. Altman, *Phys. Rev. Lett.* **110**, 067204 (2013).
  - <sup>12</sup> D. A. Huse, R. Nandkishore, and V. Oganesyan, *Physical Review B* **90**, 174202 (2014).
  - <sup>13</sup> M. Serbyn, Z. Papić, and D. A. Abanin, *Physical review letters* **111**, 127201 (2013).
  - <sup>14</sup> V. Ros, M. Müller, and A. Scardicchio, *Nucl. Phys. B* **891**, 420 (2015).
  - <sup>15</sup> J. Z. Imbrie, arXiv preprint arXiv:1403.7837 (2014).
  - <sup>16</sup> B. Bauer and C. Nayak, *Journal of Statistical Mechanics: Theory and Experiment* **2013**, P09005 (2013).
  - <sup>17</sup> A. Chandran, I. H. Kim, G. Vidal, and D. A. Abanin, *Physical Review B* **91**, 085425 (2015).
  - <sup>18</sup> M. Schreiber, S. S. Hodgman, P. Bordia, H. P. Lüschen, M. H. Fischer, R. Vosk, E. Altman, U. Schneider, and I. Bloch, arXiv:1501.05661 (2015).
  - <sup>19</sup> J. Smith, A. Lee, P. Richerme, B. Neyenhuis, P. W. Hess, P. Hauke, M. Heyl, D. A. Huse, and C. Monroe, arXiv:1508.07026 (2015).
  - <sup>20</sup> S. Ghosh, R. Parthasarathy, T. Rosenbaum, and G. Aeppli, *Science* **296**, 2195 (2002).
  - <sup>21</sup> G. Feher, *Physical Review* **114**, 1219 (1959).
  - <sup>22</sup> M. Serbyn, Z. Papić, and D. A. Abanin, *Physical review letters* **110**, 260601 (2013).
  - <sup>23</sup> A. Chandran, V. Khemani, C. Laumann, and S. Sondhi, *Physical Review B* **89**, 144201 (2014).
  - <sup>24</sup> A. Abragam and M. Goldman, *Nuclear Magnetism: Order and Disorder* (Oxford University Press, 1982).
  - <sup>25</sup> Empirically a glassy atomic structure is necessary to obtain significant hyper-polarization. The reason is not entirely established, but such a structure presumably helps to ensure a homogeneous dilution of radicals (and to prevent the clustering of radicals at lower-dimensional grain boundaries).
  - <sup>26</sup> J. H. Ardenkjær-Larsen, B. Fridlund, A. Gram, G. Hansson, L. Hansson, M. H. Lerche, R. Servin, M. Thaning, and K. Golman, *Proc. Natl. Acad. Sci. U.S.A.* **100**, 10158 (2003).
  - <sup>27</sup> K. Golman, M. Lerche, R. Pehrson, J. H. Ardenkjær-Larsen, *et al.*, *Cancer Res.* **66**, 10855 (2006).
  - <sup>28</sup> B. Provotorov, *SOVIET PHYSICS JETP-USSR* **14**, 1126 (1962).
  - <sup>29</sup> L. Lumata, A. K. Jindal, M. E. Merritt, C. R. Malloy, A. D. Sherry, and Z. Kovacs, *J. Am. Chem. Soc.* **133**, 8673 (2011).
  - <sup>30</sup> F. Kurdzesau, B. van den Brandt, A. Comment, P. Hautle, S. Jannin, J. van der Klink, and J. Konter, *J. Phys. D: Appl. Phys.* **41**, 155506 (2008).
  - <sup>31</sup> M. Borghini, *Phys. Rev. Lett.* **20**, 419 (1968).
  - <sup>32</sup> A. De Luca and A. Rosso, *Phys. Rev. Lett.* **115**, 080401 (2015).
  - <sup>33</sup> Y. Hovav, A. Feintuch, and S. Vega, *J. Magn. Reson.* **207**, 176 (2010); **214**, 29 (2012); *Phys. Chem. Chem. Phys.* **15**, 188 (2013).
  - <sup>34</sup> A. Karabanov, D. Wiśniewski, I. Lesanovsky, and W. Köckenberger, *Physical Review Letters* **115**, 020404 (2015), arXiv:1503.04357 [quant-ph].
  - <sup>35</sup> S. Colombo Serra, M. Filibian, P. Carretta, A. Rosso, and F. Tedoldi, *Phys. Chem. Chem. Phys.* **16**, 753 (2014).
  - <sup>36</sup> F. Buccheri, A. De Luca, and A. Scardicchio, *Phys. Rev. B* **84**, 094203 (2011).
  - <sup>37</sup> Explicitly, the energy shifts are chosen as  $\Delta_i = \Delta\omega_e \left( \frac{2i-N-1}{N} \right)$  with  $i = 1, \dots, N$ .
  - <sup>38</sup> M. Filibian, S. C. Serra, M. Moscardini, A. Rosso, F. Tedoldi, and P. Carretta, *Phys. Chem. Chem. Phys.* **16**, 27025 (2014).
  - <sup>39</sup> F. Petruccione and H.-P. Breuer, *The theory of open quantum systems* (Oxford Univ. Press, 2002).
  - <sup>40</sup> H. Jóhannesson, S. Macholl, and J. H. Ardenkjær-Larsen, *J. Magn. Reson.* **197**, 167 (2009).
  - <sup>41</sup> Indeed, the electron spin-flips induced by the bath are the slowest process and fully determine the polarization time,  $T_{pol} = \frac{N_n}{N_e} T_{1e}$ .
  - <sup>42</sup> S. C. Serra, A. Rosso, and F. Tedoldi, *Physical Chemistry Chemical Physics* **14**, 13299 (2012).
  - <sup>43</sup> S. Serra Colombo, A. Rosso, and F. Tedoldi, *Phys. Chem. Chem. Phys.* **15**, 8416 (2013).
  - <sup>44</sup> A. Karabanov, A. van der Drift, L. J. Edwards, I. Kuprov, and W. Köckenberger, *Phys. Chem. Chem. Phys.* **14**, 2658 (2012).
  - <sup>45</sup> A. L. Burin, arXiv preprint cond-mat/0611387 (2006).
  - <sup>46</sup> N. Y. Yao, C. R. Laumann, S. Gopalakrishnan, M. Knap, M. Mueller, E. A. Demler, and M. D. Lukin, *Physical review letters* **113**, 243002 (2014).
  - <sup>47</sup> M. Filibian, S. C. Serra, M. Moscardini, A. Rosso, F. Tedoldi, and P. Carretta, *Phys. Chem. Chem. Phys.* **16**, 27025 (2014).

## Appendix A: Borghini model with interactions

In this appendix, we provide a general method to determine the two parameters  $\beta_s, h$  conjugate to the two conserved quantities of the Hamiltonian  $\hat{H}$  in (9). In the dynamics described by the master equation (11), the system exchanges simultaneously energy and magnetization every time a spin is flipped by the reservoir or the microwaves. We can compute explicitly the joint probability distribution  $P(\Omega, S)$  of the energy and magnetization variation within a time interval  $[t, t + \delta t]$ :

$$P(\Omega, S) = \sum_{nn'} \delta[\Omega - (\epsilon_n - \epsilon_{n'})] \delta[S - (s_z^n - s_z^{n'})] P_{n' \rightarrow n}^{\delta t} p_{n'}(t), \quad (\text{A1})$$

where  $P_{n' \rightarrow n}^{\delta t}$  is the probability of passing from  $n' \rightarrow n$  in a time  $\delta t$ . In the limit  $\delta t \rightarrow 0$ , we have therefore for  $n \neq n'$ ,  $P_{n' \rightarrow n}^{\delta t} = W_{n' \rightarrow n} \delta t$  and  $P_{n \rightarrow n}^{\delta t} = 1 - \sum_{n' \neq n} P_{n \rightarrow n'} = 1 - \sum_{n' \neq n} W_{n \rightarrow n'} \delta t$ . Replacing in (A1), we arrive at  $P(\Omega, S, t) = P_{n \rightarrow n} \delta(\Omega) \delta(S) + \delta t p(\Omega, S, t)$  with

$$p(\Omega, S, t) = \sum_{\substack{n, n' \\ n \neq n'}} \delta[\Omega - (\epsilon_n - \epsilon_{n'})] \delta[S - (s_z^n - s_z^{n'})] W_{n' \rightarrow n} p_{n'}(t), \quad (\text{A2})$$

while the term  $P_{n \rightarrow n}$  does not contribute to the average of  $\Omega$  and  $S$ . In the large time limit  $p_n(t) \rightarrow p_n^{\text{stat}}$ ; moreover, using the rates in (12, 16) and the integral representation of the  $\delta$ -function, we have

$$\sum_{n \neq n'} \delta[\Omega - (\epsilon_n - \epsilon_{n'})] \delta[S - (s_z^n - s_z^{n'})] W_{n, n'}^{\text{bath}} p_{n'}^{\text{stat}} = \sum_{j=1}^N \int \frac{du}{2\pi} \frac{dv}{2\pi} e^{iu\Omega + ivS} \frac{4h_\beta(-\Omega)}{T_{1e}} \chi_{jj}(u, v), \quad (\text{A3})$$

where  $\chi_{jj}(u, v)$  is defined in (19) and we used rotational symmetry around the  $z$ -axis. Analogously for the microwave rate, we obtain

$$\sum_{n \neq n'} \delta[\Omega - (\epsilon_n - \epsilon_{n'})] \delta[S - (s_z^n - s_z^{n'})] W_{n, n'}^{\text{MW}} p_{n'}^{\text{stat}} = \sum_{ij} \int \frac{du}{2\pi} \frac{dv}{2\pi} e^{iu\Omega + ivS} \frac{4\omega_1^2 T_{2e}}{1 + T_{2e}^2 (\Omega - \omega_{\text{MW}} S)^2} \chi_{ij}(u, v). \quad (\text{A4})$$

Note that in order to write Eqs. (A3, A4), we used explicitly that  $|n\rangle$  is a simultaneous eigenstate of  $\hat{H}$  and  $\hat{S}_z$ : so this derivation only holds for the conserved quantities of the model.

Let us introduce the Fourier transform of the correlation function

$$\chi_{ij}(\Omega, S) = \int \frac{du}{2\pi} \frac{dv}{2\pi} e^{i(\Omega u + S v)} \chi_{ij}(u, v), \quad (\text{A5})$$

with which, we can rewrite equation (A2) as

$$p_{\text{stat}}(\Omega, S) = \frac{4h_\beta(-\Omega)}{T_{1e}} \sum_j \chi_{jj}(\Omega, S) + \frac{4\omega_1^2 T_{2e}}{1 + T_{2e}^2 (\Omega - \omega_{\text{MW}} S)^2} \sum_{ij} \chi_{ij}(\Omega, S). \quad (\text{A6})$$

Imposing that the energy and magnetization flows vanish in the stationary state we find two equations

$$\int dS d\Omega p(\Omega, S) \Omega = 0, \quad \int dS d\Omega p(\Omega, S) S = 0. \quad (\text{A7})$$

If we assume that the stationary state is effectively thermal, in agreement with (17), i.e.,  $p_n^{\text{stat}} = e^{-\beta_s(\epsilon_n + h s_{z,n})} / Z$ , Eqs. (A7) suffice to determine the two parameters  $\beta_s, h$ . The essential ingredient is the correlation function  $\chi_{ij}(u, v)$ , which is derived in the next appendix.

## Appendix B: Perturbative calculation of the correlation function in the mean-field model

We now compute the correlation function  $\chi_{ij}(u, v)$  to second order in the dipolar interaction strength  $U$ . It is analyzed in the mean-field model defined in (9), in the thermodynamic limit  $N \rightarrow \infty$ . We keep the inhomogeneities

$\Delta_i$  finite and arbitrary. As the nuclear spin only slightly perturbs the electron spin Hamiltonian, we can neglect it in the estimation of  $\beta_s$  and  $h$  and focus on the subsystem of interacting electron spins:

$$\hat{H}_e(h) = \sum_{i=1}^N (\omega_e + h + \Delta_i) \hat{S}_z^i + \sum_{i < j} U_{ij} (\hat{S}_+^i \hat{S}_-^j + \hat{S}_-^i \hat{S}_+^j) = \hat{H}_0 + \hat{V}, \quad (\text{B1})$$

where  $\hat{H}_0$  is the non-interacting Hamiltonian, and  $\hat{V}$  describes the dipolar couplings  $U_{ij}$  between electron spins, which are Gaussian random variables with covariance matrix

$$\overline{U_{ij} U_{kl}} = \frac{U^2}{N} \delta_{ik} \delta_{jl}. \quad (\text{B2})$$

Note that, at order  $U^2$ , the correlation functions for different spins will be decoupled after averaging because of (B2), i.e.,  $\chi_{ij}(\Omega, S) = \delta_{ij} \chi_{ii}(\Omega, S) + o(U^2)$ . Thus, we can just restrict ourselves to the calculation of the dynamical correlation function  $\chi_{jj}(u, v)$  of a single-spin  $j$ . It can be simplified as

$$\chi_{jj}(u, v) = \frac{e^{i(v-hu)} \Gamma_+^j(u, h) + e^{-i(v-hu)} \Gamma_-^j(-u, h)}{4} \quad (\text{B3})$$

by introducing the  $S_+^j S_-^j$  correlators

$$\Gamma_{\pm}^j(u, h) = Z^{-1} \text{Tr}[e^{-(\beta_s - iu)\hat{H}_e(h)} \hat{S}_{\pm}^j e^{-iu\hat{H}_e(h)} \hat{S}_{\mp}^j]. \quad (\text{B4})$$

For simplicity, in the following we will keep tacit the dependence on  $h$ , since it simply amounts to changing  $\omega_e \rightarrow \omega_e + h$  in  $\hat{H}_e(0)$ . In order to take advantage of the path integral formalism, we perform a Wick rotation and define  $C_{\pm}^i(\tau) = \Gamma_{\pm}^i(-i\tau)$ . From the cyclicity of the trace, we deduce  $C_-^i(\tau) = C_+^i(\beta_s - \tau)$ , and we can thus restrict ourselves to calculating  $C_+^i(\tau)$ . We introduce the evolution operator in the interaction picture as  $\hat{U}_{\tau} = e^{\tau\hat{H}_0} e^{-\tau\hat{H}}$ , so that

$$\frac{d\hat{U}_{\tau}}{d\tau} = \hat{H}_0 \hat{U}_{\tau} - e^{\tau\hat{H}_0} \hat{H}_e e^{-\tau\hat{H}_0} \hat{U}_{\tau} = -\hat{V}_I(\tau) \hat{U}_{\tau}, \quad (\text{B5})$$

where  $\hat{V}_I(\tau) = e^{\tau\hat{H}_0} \hat{V} e^{-\tau\hat{H}_0}$ . Integrating this last equation over  $[0, \tau]$  and re-injecting the resulting equation to itself, we get the second order expansion

$$e^{-\tau\hat{H}} = e^{-\tau\hat{H}_0} - \int_0^{\tau} dt' e^{(t'-\tau)\hat{H}_0} \hat{V} e^{-t'\hat{H}_0} + \int_0^{\tau} dt' \int_0^{t'} dt'' e^{(t'-\tau)\hat{H}_0} \hat{V} e^{(t''-t')\hat{H}_0} \hat{V} e^{-t''\hat{H}_0}. \quad (\text{B6})$$

In order to keep track of all the terms in the expansion in  $U$ , we write  $\hat{V} \rightarrow \epsilon \hat{V}$ . We can expand the reduced partition function and the correlation function as

$$\frac{Z}{Z_0} = (1 + \epsilon z^{(1)} + \epsilon^2 z^{(2)}), \quad (\text{B7})$$

$$\frac{C_+^i(\tau) Z}{Z_0} = c_+^{i,(0)}(\tau) + \epsilon c_+^{i,(1)}(\tau) + \epsilon^2 c_+^{i,(2)}(\tau), \quad (\text{B8})$$

where  $Z_0$  is the non-interacting ( $U_{ij} = 0$ ) partition function. Then, we have the expansion

$$\overline{C_+^i} = c_+^{i,(0)}(\tau) (1 + (\overline{z^{(1)}})^2 - \overline{z^{(2)}}) - \overline{z^{(1)} c_+^{i,(1)}(\tau)} + \overline{c_+^{i,(2)}(\tau)}, \quad (\text{B9})$$

where the overline represents the average taken over the distribution of the dipolar couplings  $U_{ij}$ , with fixed values of the  $\Delta_i$ 's. Note that  $\overline{\hat{V}} = 0$  so the first non-vanishing correction is quadratic. Moreover  $z^{(1)}$  vanishes identically since  $\langle n_0 | V | n_0 \rangle = 0$  for any eigenstate  $|n_0\rangle$  of  $\hat{H}_0$ . After some algebra, the calculation up to second order of each term leads to the expression

$$\overline{C_+^i(\tau)} = c_+^{i,(0)}(\tau) + \frac{U^2}{N} \sum_{l \neq i} \frac{d}{d\Delta_i} \left[ \frac{c_+^{i,(0)}(\tau) - c_+^{l,(0)}(\tau)}{\Delta_i - \Delta_l} \right], \quad (\text{B10})$$

where

$$c_+^{i,(0)}(\tau) = \frac{\text{Tr}[e^{-(\beta_s - \tau)(\omega_e + \Delta_i)S_z} S_+^i e^{-\tau(\omega_e + \Delta_i)S_z} S_-^i]}{\text{Tr}[e^{-\beta_s(\omega_e + \Delta_i)S_z}]} = \frac{e^{\tau(\omega_e + \Delta_i)}}{1 + e^{\beta_s(\omega_e + \Delta_i)}}. \quad (\text{B11})$$

A simpler way to derive Eq. (B10) is to note, by simple power counting, that at order  $U^2$ , the perturbation in  $\overline{C_+^i(\tau)}$  must consist in additive contributions from all spins  $l \neq i$ . The term inside the sum in (B10) can then be obtained by solving exactly the case  $N = 2$  for an arbitrary value of the coupling  $U_{12}$  in (B1) and expanding up to the order  $U_{12}^2$ .

Note that the expression (B11) allows us also to compute the local polarizations:

$$P_i = 2 \text{Tr}[S_z^i \rho] = \text{Tr}[S_+^i S_-^i \rho] - \text{Tr}[S_-^i S_+^i \rho] = \overline{C_+^i(0)} - \overline{C_-^i(0)} = P_i^0 + \frac{U^2}{N} \sum_{l \neq i} \frac{d}{d\Delta_i} \left[ \frac{P_i^0 - P_l^0}{\Delta_i - \Delta_l} \right], \quad (\text{B12})$$

where  $P_i^0 = -\tanh\left(\frac{\beta_s(\omega_e + \Delta_i)}{2}\right)$  are the non-interacting polarizations for  $U = 0$ .

Performing back the Wick rotation  $\tau = iu$  and replacing  $\omega_e \rightarrow \omega_e + h$  in (B10) and (B11), we obtain  $\Gamma_{\pm}^i(u, h)$

$$\Gamma_+^i(u, h) = \frac{e^{iu(\omega_e + h + \Delta_i)}}{1 + e^{\beta_s(\omega_e + h + \Delta_i)}} + \frac{U^2}{N} \sum_{l \neq i} \frac{d}{d\Delta_i} \left[ \frac{\frac{e^{iu(\omega_e + h + \Delta_i)}}{1 + e^{\beta_s(\omega_e + h + \Delta_i)}} - \frac{e^{iu(\omega_e + h + \Delta_l)}}{1 + e^{\beta_s(\omega_e + h + \Delta_l)}}}{\Delta_i - \Delta_l} \right], \quad (\text{B13})$$

$$\Gamma_-^i(u, h) = \frac{e^{(\beta_s - iu)(\omega_e + h + \Delta_i)}}{1 + e^{\beta_s(\omega_e + h + \Delta_i)}} + \frac{U^2}{N} \sum_{l \neq i} \frac{d}{d\Delta_i} \left[ \frac{\frac{e^{(\beta_s - iu)(\omega_e + h + \Delta_i)}}{1 + e^{\beta_s(\omega_e + h + \Delta_i)}} - \frac{e^{(\beta_s - iu)(\omega_e + h + \Delta_l)}}{1 + e^{\beta_s(\omega_e + h + \Delta_l)}}}{\Delta_i - \Delta_l} \right]. \quad (\text{B14})$$

### Appendix C: Equations for $\beta_s$ and $h$ in the mean-field model

Using (B11) and (A5), the correlation  $\chi_{jj}^{U=0}(\Omega, S)$  in the non-interacting case is:

$$\chi_{jj}^{U=0}(\Omega, S) = \frac{\delta(S-1)h\beta_s(\omega_e + h + \Delta_j)\delta(\Delta_j - \Omega + \omega_e)}{4} + \frac{\delta(S+1)h\beta_s(-\omega_e - h - \Delta_j)\delta(\Delta_j + \Omega + \omega_e)}{4}. \quad (\text{C1})$$

Using (A6) and (A7), the integration over  $S, \Omega$  leads to the equations which fix  $h$  and  $\beta_s$ :

$$\sum_j \kappa(\omega_e + \Delta_j) = 0, \quad (\text{C2})$$

$$\sum_j (\omega_e + \Delta_j) \kappa(\omega_e + \Delta_j) = 0, \quad (\text{C3})$$

where  $\kappa(\omega)$  is defined in (21). Eqs. (20) are recovered in the large  $N$  limit, where the sums over  $j$  can be converted into integrals over the distribution of inhomogeneities,  $f(\Delta)$ . Then, since (B10) is a linear combination of the functions the  $c_+^{i,(0)}(\tau)$ , to order  $U^2$  the equations simply become

$$\sum_j \left[ \kappa(\omega_e + \Delta_j) + \frac{U^2}{N} \sum_{l \neq j} \frac{d}{d\Delta_j} \left( \frac{\kappa(\omega_e + \Delta_j) - \kappa(\omega_e + \Delta_l)}{\Delta_j - \Delta_l} \right) \right] = 0, \quad (\text{C4})$$

$$\sum_j \left[ (\omega_e + \Delta_j) \kappa(\omega_e + \Delta_j) + \frac{U^2}{N} \sum_{l \neq j} \frac{d}{d\Delta_j} \left( \frac{(\omega_e + \Delta_j) \kappa(\omega_e + \Delta_j) - (\omega_e + \Delta_l) \kappa(\omega_e + \Delta_l)}{\Delta_j - \Delta_l} \right) \right] = 0. \quad (\text{C5})$$